Desalination and Water Treatment
www.deswater.com

doi:10.5004/dwt.2019.24256

156 (2019) 46–51
July

Fabrication of MoS_2/polyelectrolyte composite membrane on ceramic tube with enhanced nanofiltration performance

Jingyuan Zhou[a], Zhenping Qin[a,*], Tongtong Liu[a], Yue Ma[a], Quanfu An[a], Hongxia Guo[b,*]

[a]*Beijing Key Laboratory for Green Catalysis and Separation, College of Environmental and Energy Engineering, Beijing University of Technology, Beijing 100124, China, email: zhenpingq@bjut.edu.cn (Z. Qin)*
[b]*College of Materials Science and Engineering, Beijing University of Technology, Beijing 100124, China, email: hxguo@bjut.edu.cn. (H. Guo)*

Received 27 July 2018; Accepted 19 February 2019

ABSTRACT

In order to improve the separation performance of the nanofiltration (NF) membranes, numerous inorganic components have been introduced into polymer membranes. Molybdenum disulfide (MoS_2) is an emerging graphene-like nanomaterials, which has many advantages, and expected to have novel applications in the NF fields. Herein, this work the PDDA modified MoS_2 nanosheets were prepared, which showed better dispersion in aqueous solution, and the modified PDDA@MoS_2 displayed higher compatibility with the polyelectrolyte. Then, the prepared PDDA@MoS_2 nanosheets was introduced into polyelectrolyte membrane through LbL self-assembled method to get an organic/inorganic composite NF membrane with ceramic tube as substrate. The membrane was used to NF separation of dyes from aqueous solution. The results suggested that the membrane flux increased first and then decreased with increasing PDDA@MoS_2 nanosheets concentration, while the rejection remained almost constant. Specifically, under optimum condition, the prepared $(PSS/PDDA\text{-}MoS_2)_{4.5}$ ceramic composite membrane showed 97.2% of rejection for 0.20 g/L methyl blue dye solution, along with flux of 163.2 $L \cdot m^{-2} \cdot h^{-1} \cdot MPa^{-1}$, which was ~2.4 times compared with pure $(PSS/PDDA)_{4.5}$ membrane without sacrificing rejection.

Keywords: MoS_2 nanosheets; Ceramic membrane; Nanofiltration

1. Introduction

While the global water resource is faced with water shortage, the pollution from the waste water is becoming more serious due to population growth, industrialization and urbanization [1–4]. Nanofiltration (NF) technology has attracted growing concern due to its advantages, such as high efficiency, energy savings and being environmentally friendly [5]. Presently, most of nanofiltration membranes are mainly prepared by organic polymers, including cellulose acetate, polyamide, sulfonated polyethersulfone, sulfonated polysulfone, polyvinyl alcohol, polyphenylene oxide, polyethylenimine, polyacrylonitrile, and so on [6–8]. Although these membranes show good rejection toward various molecules, the performances are still unsatisfactory for industrial application because of the poor mechanical strength and intolerance with acid and alkali [9,10]. The inorganic ceramic membranes are particularly suitable for the purification of contaminated water since they possess high thermal, chemical and mechanical stabilities [11]. Some of nanofiltration membranes have been fabricated on ceramic substrates and exhibited relatively high rejection towards dyes molecules in aqueous solution, but there is still necessary to improve the permeable flux for the extensive utilization [12,13].

Molybdenum disulfide (MoS_2) as an emerging graphene-like nanomaterials has shown superiority in performance enhancement of NF membrane. In our previous work [14], the polyelectrolyte modified PDDA@MoS_2 nanosheets have been prepared and incorporated into polyelectrolyte multi layers (PEMs) through layer-by-layer (LbL) method to get a PDDA@MoS_2-PDDA/PSS hybrid membrane on poly-

---

*Corresponding author.

1944-3994 / 1944-3986

acrylonitrile (PAN) substrate. The obtained hybrid membrane displayed 2.3 times flux than that of pure PDDA/PSS polyelectrolyte membrane without sacrificing the rejection. Also, due to the good dispersive stability in aqueous solution, the modified PDDA@MoS_2 nanosheets have good compatibility with the polyelectrolytes, thereby the hybrid membrane showed excellent operation stability in NF separation of dyes from water.

The tubular ceramic membrane composited by a hybrid active layer is a more attracting strategy to a high NF performance membrane. In this work, a composite MoS_2/polyelectrolytes ceramic membrane was fabricated with tubular ceramic as substrate. The prepared membrane was used for nanofiltration separation of dye, such as methyl blue (MB), from water solution. Such ceramic composite membranes exhibited great potentials in practical applications of water purification through nanofiltration process.

2. Experimental section

2.1. Materials and chemicals

Tubular ceramic substrate with 42.0 mm long and 8.5 mm inner and 13.5 outer diameters were supplied by Jiexi Lishun Technology Co., Ltd. (Guangdong, China). Poly (diallyldimethylammonium chloride) (PDDA, M_w = 750,000), Poly (sodium 4-styrenesulfonate) (PSS, M_w = 1,000,000), silane coupling agent (3-aminopropyl-trimethoxysilane), ammonium molybdate tetrahydrate ($(NH_4)_6Mo_7O_{24}\cdot 4H_2O$), and thiourea ($CH_4N_2S$) were all purchased from Sigma-Aldrich Co. (USA). NaOH, ethanol and methyl blue (MB) were obtained from Beijing Chemical Factory (Beijing, China). De-ionized (DI) water with a resistance of 18.2 MΩ was used in all experiments. The chemicals were used as received without further purification.

2.2. Synthesis of PDDA modified MoS_2 (PDDA@MoS_2) nanosheet

PDDA modified MoS_2 (PDDA@MoS_2) nansheets were prepared according to our previous method [14]. Briefly, the mixed aqueous solution of 8.0 mL 62.5 g/L of ammonium molybdate tetrahydrate ($(NH_4)_6Mo_7O_{24}\cdot 4H_2O$) and 125.0 g/L of thiourea (CH_4N_2S) was added to 10 mL 100.0 g/L of PDDA aqueous solution under continuous stirring for 24 h. After that, the mixed solution was transferred into a 25 mL Teflon-lined stainless steel autoclave and maintained at 220°C for 18 h. The reaction system was then allowed to cool to room temperature. The product was taken out and thoroughly washed with water and absolute ethanol, and dried at 60°C to get PDDA@MoS_2 nanosheets.

2.3. Preparation of PDDA@MoS_2 polyelectrolyte composite membrane on ceramic tube

The tubular ceramic substrate was first pre-treated using the method of references [15–17], which is the general way to pre-treat the ceramic tubular substrate. Specifically, the tube was immersed in a mixture of 8.0 g/L silane coupling agents and 95 wt. % ethanol aqueous solution. Then, as shown in Fig. 1, the pre-treated tubular ceramic substrate was immersed into 3.0 g/L PSS solution for 20 min, after taken out and rinsed by de-ionized water. Subsequently, the membrane was immersed into 3.0 g/L PDDA solution which contained 0.2 g/L of PDDA@MoS_2 nanosheets for 20 min. The membrane was taken out and rinsed with de-ionized water again. The steps were repeated for three times to obtain the $(PSS/PDDA\text{-}MoS_2)_{4.5}$ ceramic composite membrane. As a comparison, the $(PSS/PDDA)_{4.5}$ polyelectrolytes membrane was prepared using the similar method on the tubular ceramic substrate [18,19], but none of the PDDA@MoS_2 nanosheets were added.

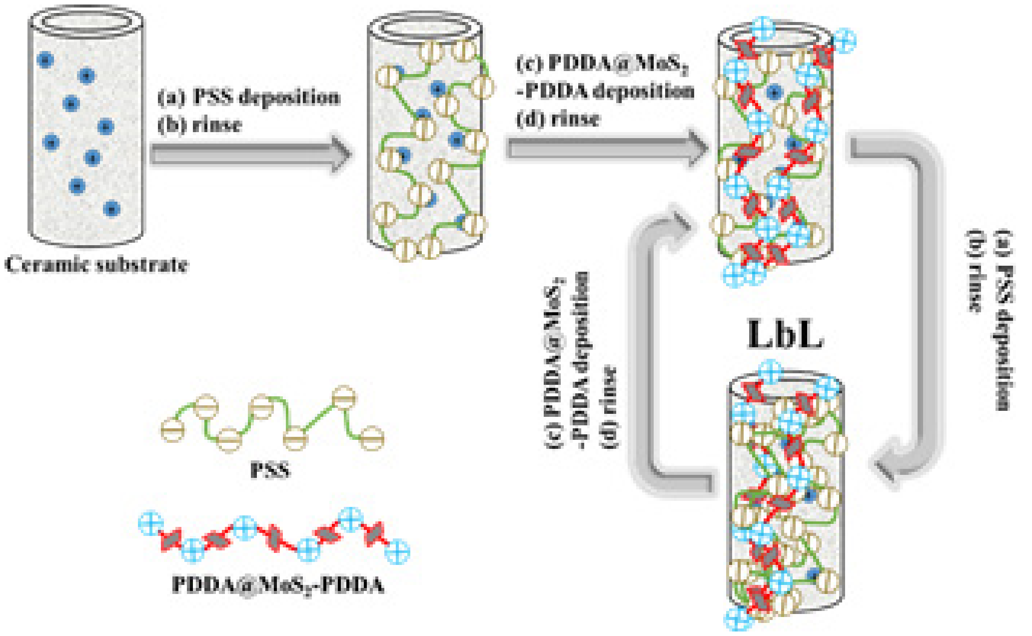

Fig. 1. Schematic illustration of the preparation of (PSS/PDDA-MoS_2) 4.5 composite membrane on tubular ceramic substrate.

2.4. Characterizations

The scanning electron microscope (SEM) images were observed on a SU8020 instrument (Hitachi, Japan), prior to observations, all samples were coated with gold nanoparticles in vacuum to increase their conductivity. Elemental compositions of the membranes were analyzed using an energy dispersive spectroscopy (EDS) apparatus along with SEM. The water contact angle was measured using a contact-angle measurement apparatus (DSA-100, KRUSS, Germany) based on the sessile-drop method. To minimize investigation error, five random locations of each membrane were measured and the average value was recorded.

2.5. Nanofiltration performance

Nanofiltration performance was evaluated using a cross flow NF system which contained membrane cell, plunger pump, pressure gauge, and solution vessel as our previous work [8]. The nanofiltration membrane was loaded into the membrane cell for filtration with effective membrane area of 9.6 cm^2. The feed solution was pressurized with a plunger pump. The filtration pressure was maintained at 0.20 MPa. During the NF process, the concentrate was recirculated to the feed vessel while permeate was collected in permeate vessel. The flux J (L/m^2·h·MPa) was calculated by: $J = V/t \times A \times P$, where V (L) is volume of the permeate sample, t (h) is time for collecting sample, A is the membrane area (m^2), P is operation pressure (MPa). The solute rejection rate R was calculated by: $R = (1 - C_p/C_F) \times 100\%$, where C_p is the solute concentration in the permeate and C_F represents solute concentration in the feed. The dye concentrations were measured by an ultraviolet-visible spectrophotometer (UV-3200, Shanghai Mapada Instruments Co. Ltd., China) at the maximal absorption wavelength of the dye. In all filtration experiments, at least three membrane samples were taken.

3. Results and discussion

3.1. The morphology and wettability of the PSS/PDDA-MoS$_2$ composite membrane

The PSS/PDDA-MoS$_2$ composite membrane was prepared on tubular ceramic substrate through a typical LbL self-assembly method. The surface morphology and composition of the (PSS/PDDA-MoS$_2$)$_{4.5}$ composite membrane were characterized by SEM and EDS. As shown in Fig. 2a, the bared tubular ceramic substrate displayed porous surface composed of uniformly Al$_2$O$_3$ crystalline particles. After the PSS/PDDA-MoS$_2$ was assembled on the tubular ceramic substrate, the SEM image in Fig. 2b indicated that the porous substrate was fully covered by much denser (PSS/PDDA-MoS$_2$)$_{4.5}$ composite layer, and there was no obvious defects on the surface. The existence of Mo element was confirmed by EDS mapping image (inset of Fig. 2b), which indicated that the PDDA@MoS$_2$ nanosheets were dispersed uniformly in polyelectrolytes multi layers.

The water contact angle (WCA) are widely used to assess the wettability of membrane surfaces. Fig. 2c indicated that the WCA of the (PSS/PDDA)$_{4.5}$ membrane on ceramic substrate was 31.1°, while that of the (PSS/PDDA-MoS$_2$)$_{4.5}$ composite membrane in Fig. 2d was 43.2°, suggesting that the MoS$_2$ nanosheets weakened the hydrophilicity of the polyelectrolyte membrane. This was due to that the introduction of PDDA@MoS$_2$ nanosheets into PEMs would

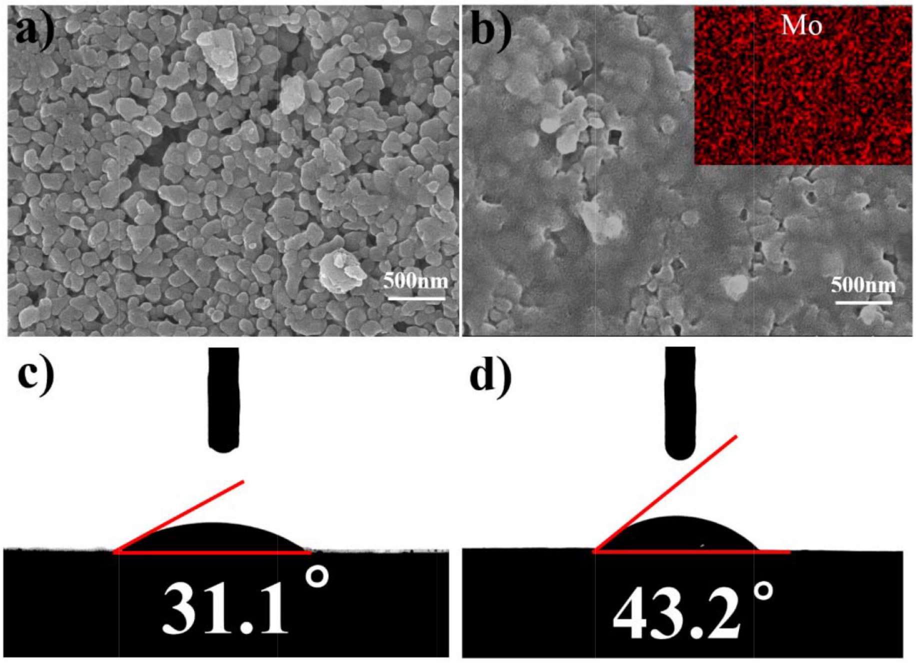

Fig. 2. SEM images of surface morphologies of a) ceramic substrate, b) tubular hybrid membrane. Inset of (b) was EDS mapping image of Mo element; The corresponding water contact angles of c) (PSS/PDDA)4.5 polyelectrolyte membrane, d) (PSS/PDDA-PDDA@MoS$_2$) 4.5 ceramic composite membrane (Preparation conditions: PDDA of 4.0 g/L, PSS of 3.0 g/L, PDDA@MoS$_2$ of 0.20 g/L).

have stronger interaction with hydrophilic groups of polyelectrolyte chains, leading to a more compact surface and a decreased water contact angle.

3.2. Nanofiltration performance of PDDA@MoS$_2$ hybrid membranes

The as-prepared PSS/PDDA-MoS$_2$ ceramic composite membrane were used in NF separation of 0.20 g/L methyl blue (MB) aqueous solution at room temperature. The effect of bilayer number on the NF performance of the hybrid membrane is shown in Fig. 3. It was noted that the rejection of MB increased while the flux decreased with increasing the number of bilayer, indicating a trade-off effect. When 1.5 bilayer of (PSS/PDDA)$_{1.5}$-MoS$_2$ membrane was assembled, the flux was 258.4 L·m^{-2}·h^{-1}·MPa^{-1} and the rejection was 85.5%. With the assembled bilayer increasing to 4.5, the rejection of MB increased to 97.8%, along with flux of 163.2 L·m^{-2}·h^{-1}·MPa^{-1}. When the assembled bilayer was further increased to 5.5, but the flux drops to 68.0 L·m^{-2}·h^{-1}·MPa^{-1}, while the rejection showed almost unchanged. This was attributed to that the thickness of the active layer increased with increasing the number of bilayer leading to a larger transport resistance and decreased flux. Therefore, 4.5 bilayers was chosen for preparation of subsequent PSS/PDDA-MoS$_2$ ceramic composite membrane.

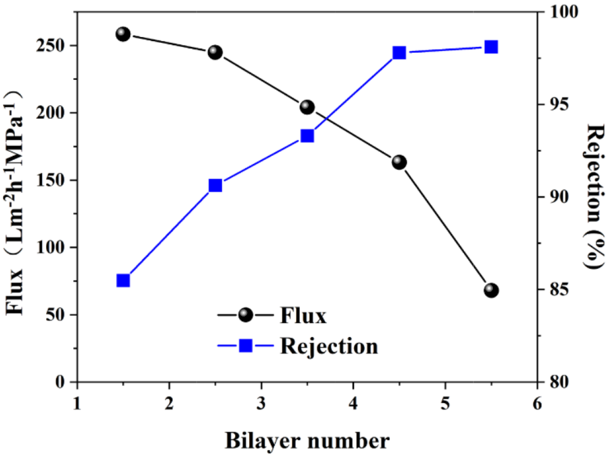

Fig. 3. Effect of number of bilayer on the NF performance (Membrane preparation condition: PDDA of 3.0 g/L, PSS of 3.0 g/L, 0.20 g/L of PDDA@MoS$_2$; NF operating condition: 0.20 MPa, 0.20 g/L MB aqueous solution).

Then, the effects of PSS and PDDA concentration on NF performance was investigated as shown in Fig. 4. It can be seen from Fig. 4a that with increasing PSS concentration from 1.0 g/L to 5.0 g/L, the flux of (PSS/PDDA-MoS$_2$)$_{4.5}$ composite membrane dramatically decreased from 250.2 L·m^{-2}·h^{-1}·MPa^{-1} to 65.3 L·m^{-2}·h^{-1}·MPa^{-1}; while the rejection of MB increased from 95.33% to 98.87%. In addition, the NF performance of the membrane with different PDDA concentrations shown in Fig. 4b indicated that the rejection of MB increased from 95.5% to 98.4%, while the flux decreased from 190.4 L·m^{-2}·h^{-1}·MPa^{-1} to 127.1 L·m^{-2}·h^{-1}·MPa^{-1} with increasing PDDA concentration from 1.0 g/L to 5.0 g/L. This was due to that the higher polyelectrolytes concentration would induce in much denser and thicker active layer, leading to a reduced flux and enhanced rejection.

Under the optimum LbL assembly conditions, the effect of PDDA@MoS$_2$ concentration on NF separation performance is shown in Fig. 5. It can be found that the rejection and flux of the (PSS/PDDA)$_{4.5}$ polyelectrolyte membrane were 97.6% and 68.0 L·m^{-2}·h^{-1}·MPa^{-1}, respectively. The flux of the membrane showed obviously increased after introduction of PDDA@MoS$_2$ nanosheets into membrane. When the concentration of nanosheets was 0.2 g/L, the flux of the membrane significantly increased to 163.2 L·m^{-2}·h^{-1}·MPa^{-1}. But the flux decreased to 135.6 L·m^{-2}·h^{-1}·MPa^{-1} with further increasing PDDA@MoS$_2$ concentration from to 0.40 g/L, meanwhile, the rejection of membranes almost remained at 97.6%. The flux of the (PSS/PDDA-MoS$_2$)$_{4.5}$ composite membrane with 0.20 g/L of PDDA@MoS$_2$ was at least 2.4 times than that of the (PSS/PDDA)$_{4.5}$ polyelectrolytes membrane. This was consistent with the result of our previous PDDA@MoS$_2$-PDDA/PSS hybrid membrane on polyacrylonitrile (PAN) substrate [14]. This was due to that the widened interlayer spacing and plenty of defects of

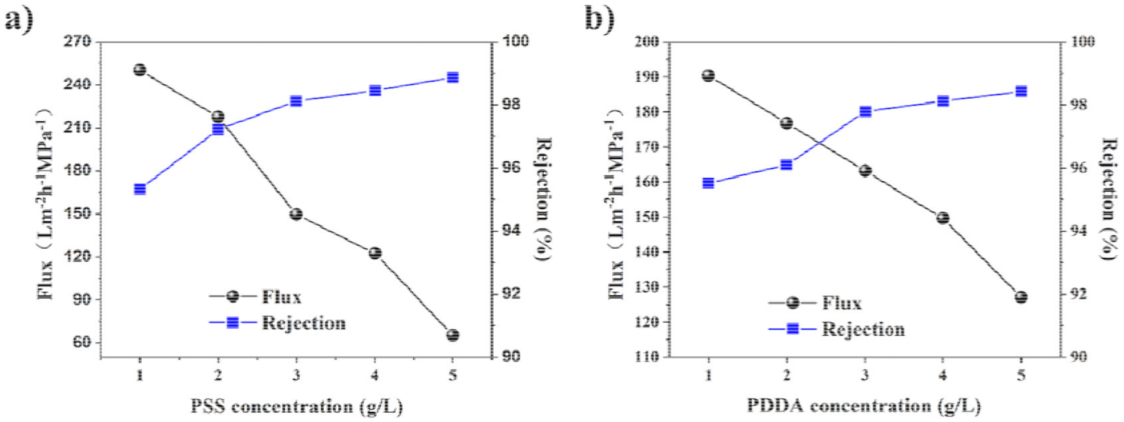

Fig. 4. Effect of (a) PSS and (b) PDDA concentration on NF performance (Preparation conditions: 4.0 g/L of PDDA and 0.40 g/L of PDDA@MoS$_2$ for (a); 3.0 g/L PSS and 0.20 g/L PDDA@MoS$_2$ for (b); operating condition: 0.20 MPa, 0.20 g/L MB aqueous solution).

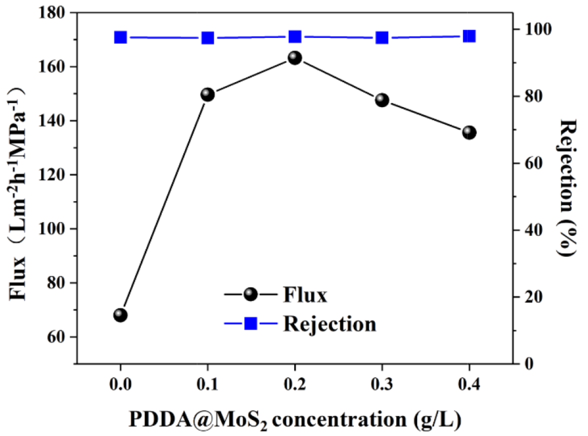

Fig. 5. Effect of PDDA@MoS_2 concentration on the nanofiltration performance. (Membrane preparation condition: PSS of 3.0 g/L, PDDA of 3.0 g/L; operating condition: 0.20 MPa, 0.20 g/L MB aqueous solution).

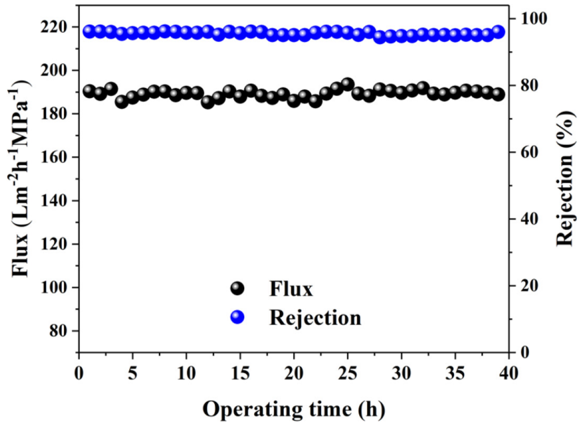

Fig. 6. The consecutive running stability of tubular PDDA@MoS_2 hybrid membrane. (Preparation conditions: PSS concentration 3.0 g/L, PDDA concentration 1.0 g/L, PDDA@MoS_2 concentration 0.20 g/L ; Operating conditions: 0.20 MPa, 0.20 g/L MB aqueous solution).

PDDA@MoS_2 contributed to the improved NF performance of the hybrid membranes [14,20]. The enlarged interlayer spacing of PDDA@MoS_2 was 11.2 Å, leaving a gallery height of 8.03 Å, which was spacial enough for water molecules to transport leading to an enhanced flux. However, further increasing the content of PDDA@MoS_2 nanosheets to more than 0.20 g/L, the stronger interaction of the inorganic nanosheet and the hydrophilic groups of polyelectrolyte chains would induce in much denser layer of the membrane resulting in reduced flux.

3.3. The consecutive NF performance of the (PSS/PDDA-MoS_2)$_{4.5}$ composite membrane

The consecutive running stability of the (PSS/PDDA-MoS_2)$_{4.5}$ ceramic composite membrane was evaluated using 0.20 g/L MB aqueous solution. As shown in Fig. 6, the flux of the membrane remained around 190.0 $L\cdot m^{-2}\cdot h^{-1}\cdot MPa^{-1}$ without almost no fluctuation even after washed with HCl water solution at pH of 2; while the rejection was maintained at about 95.7% during the running time of 39 h, indicating that the resulted (PSS/PDDA-MoS_2)$_{4.5}$ ceramic membrane showed good stability. This was ascribed to that the higher compatibility between the modified PDDA@MoS_2 nanosheets and the polyelectrolytes induced in the dispersion of PDDA@MoS_2 nanosheets in the polyelelctolytes uniformly, and that the stronger interaction between PDDA@MoS_2 and the polyelectrolytes ensured the good stability. Therefore, different with that of Bruggen's work [21], in which there occurred loss of MoS_2 in the initial 2 h filtration, the (PSS/PDDA-MoS_2)$_{4.5}$ ceramic composite membrane displayed a high stability during 39 h of running time.

For comparison, the dye removal performances in other membranes reported in the literature are summarized in Table 1. It can be noted that the nanofiltration performances of our (PSS/PDDA-MoS_2)$_{4.5}$ ceramic membrane showed comparable rejection of dyes and much higher flux. Due to the low toxicity of MoS_2 nanosheets [29], the introduction of MoS_2 nanosheets provided an efficient strategy to enhance membrane performance.

Table 1
Comparison of the NF performance of dye removal with other works reported

Membrane	Feed solution	F ($L\cdot m^{-2}\cdot h^{-1}\cdot MPa^{-1}$)	R (%)	Ref
(PDDA/GO)$_{3.0}$/PAN	Methyl blue	140.8	98.2	[22]
(PDDA/GO)$_{4.0}$/PAN	Congo red	58.4	99.0	
PEI-GO/PAA/PVA/GA	Methyl blue	8.7	99.3	[23]
ZIF-8/PES	Rose bengal	13.0	98.9	[24]
PVDF-SAN-60	Congo red	95.0	97.7	[25]
(PSS/PAH)$_{7.0}$	Glutamine	132.0	86.2	[26]
PAA/PVA/GA	Congo red	42.0	96.0	[13]
(PSS/PEI)$_{5.0}$/PAN	Humic acid	66.3	96.5	[27]
PEI/CMCNa/PP	Congo red	57.0	99.4	[28]
PDDA/PSS	Methyl blue	82.5	92	[12]
(PSS/PDDA)$_{4.5}$	Methyl blue	82.7	98.4	This work
(PSS/PDDA-MoS2)$_{4.5}$	Methyl blue	194.5	98.4	This work

4. Conclusions

In conclusion, a tubular $(PSS/PDDA\text{-}MoS_2)_{4.5}$ ceramic composite membrane was fabricated through LbL self-assembly method. It was found that the composite membrane has excellent NF performances for the dye removal from water. Under optimized conditions the prepared membrane represented a flux of 163.2 $L\cdot m^{-2}\cdot h^{-1}\cdot MPa^{-1}$ and rejection of 97.8% toward nanofiltration separation of MB from water. Furthermore, the flux of the membrane remained around 190.0 $L\cdot m^{-2}\cdot h^{-1}\cdot MPa^{-1}$, while the rejection was maintained at about 95.7% during 39 h running time. Combine with the advantages of the tubular ceramic module, this ceramic composite membrane has a great potential for NF treatment of dye effluents.

Acknowledgments

This work was financially supported by National Natural Science Foundation of China (21476005, 21878003) and the National Natural Science Fund for Innovative Research Groups (No. 51621003).

References

[1] P.C.D. Milly, K.A. Dunne, A.V. Vecchia, Global pattern of trends in stream flow and water availability in a changing climate, Nature, 438 (2005) 347–350.

[2] T. Larsen, S. Hoffmann, C. Lüthi, B. Truffer, M. Maurer, Emerging solutions to the water challenges of an urbanizing world, Science, 352 (2016) 928–933.

[3] T.I.E. Veldkamp, Y. Wada, J.C.J.H. Aerts, P. Döll, S.N. Gosling, J. Liu, Y. Masaki, T. Oki, S. Ostberg, Y. Pokhrel, Y. Satoh, H. Kim, P.J. Ward, Water scarcity hot spots travel downstream due to human interventions in the 20th and 21st century, Nat. Commun., 8 (2017) 15697.

[4] M. Hightower, S. Pierce, The energy challenge, Nature, 452 (2008) 285–286.

[5] A.W. Mohammad, Y.H. Teowa, W.L. Anga, Y.T. Chunga, D.L. Oatley-Radcliffec, N. Hila, Nanofiltration membranes review: recent advances and future prospects, Desalination, 356 (2015) 226–254.

[6] F. Zhao, Y. Li, X. Weng, Y. Mi. C. Ye Q. An, C. Gao, High-flux positively charged nanocomposite nanofiltration membranes filled with poly (dopamine) modified multi wall carbon nanotubes, Appl. Mater. Interfaces, 8 (2016) 6693–6700.

[7] H. Guo, M. Chen, Q. Liu, Z. Wang, S. Cui, G. Zhang, LbL assembly of sulfonated cyclohexanone-formaldehyde condensation polyer and poly (ethyleneimine) towards rejection of both cationic ions and dyes, Desalination, 365 (2015) 108–116.

[8] N. Wang, T. Liu, H. Shen, S. Ji, R. Zhang, J. Li, Ceramic tubular MOF hybrid membrane fabricated through in situ Layer-by-Layer self-assembly for nanofiltration, AIChE J., 62 (2016) 538–546.

[9] J. Yin, B. Deng, Polymer-matrix nanocomposite membranes for water treatment, J. Membr. Sci., 479 (2015) 256–275.

[10] R. Zhang, S. Ji, N. Wang, L. Wang, G. Zhang, J. Li, Coordination-driven in situ self-assembly strategy for the preparation of metal-organic framework hybrid membranes, Angew. Chem. Int. Ed., 53 (2014) 9775–9779.

[11] D. Zou, M. Qiu, X. Chen, Y. Fan, One-step preparation of high-performance bilayer α-alumina ultra filtration membranes via co-sintering process, J. Membr. Sci., 524 (2017) 141–150.

[12] H. Tang, S. Ji, L. Gong, H. Guo, G. Zhang, Tubular ceramic-based multilayer separation membranes using spray layer-by-layer assembly, Polym Chem., 4 (2013) 5621–5628.

[13] L. Wang, N. Wang, G. Zhang, S. Ji, Covalent cross linked assembly of tubular ceramic-based multilayer nanofiltration membranes for dye desalination, AIChE J., 59 (2013) 3834–3842.

[14] J. Zhou, Z. Qin, Y. Lu, X. Li, Q. Fu, S. Ji, N. Wang, H. Guo, MoS_2/polyelectrolytes hybrid nanofiltration (NF) membranes with enhanced permselectivity, J. Taiwan. Inst. Chem. E., 84 (2018) 196–202.

[15] Y. Zhang, N. Wang, S. Ji, R. Zhang, C. Zhao, J. Li, Metal-organic framework/poly (vinyl alcohol) nanohybrid membrane for pervaporation of toluene/n-heptane mixtures, J. Membr. Sci., 489 (2015) 144–152.

[16] A. Huang, W. Dou, J. Caro, Steam-stable zeolitic imidazolate framework ZIF-90 membrane with hydrogen selectivity through covalent functionalization, J. Am. Chem. Soc., 132 (2010) 15562–15564.

[17] P. Sae-oui, U. Thepsuawan, K. Hatthapanit, Effect of curing system on reinforcing efficiency of silane coupling agent, Polym. Test., 23 (2004) 397–403.

[18] H. Guo, Y. Ma, P. Sun, S. Cui, Z. Qin, Y. Liang, Self-cleaning and anti-fouling nanofiltration membranes-super hydrophilic multi layered polyelectrolyte/CSH composite film towards rejection of dyes, RSC Adv., 5 (2015) 63429–63438.

[19] Z. Qin, X. Ren, L. Shan, H. Guo, C. Geng, G. Zhang, S. Ji, Y. Liang, Nacrelike-structured multi layered polyelectrolyte/calcium carbonate nanocomposite membrane via Ca-incorporated layer-by-layer-assembly and CO_2-induced biomineralization, J. Membr. Sci., 498 (2016) 180–191.

[20] J. Xie, J. Zhang, S. Li, F. Grote, X. Zhang, H. Zhang, R. Wang, Y. Lei, B. Pan, Y. Xie, Controllable disorder engineering in oxygen-incorporated MoS_2 ultra thin nanosheets for efficient hydrogen evolution, J. Am. Chem. Soc., 125 (2013) 17881–17888.

[21] Y. Li, S. Yang, K. Zhang, B.V. Bruggen, Thin film nanocomposite reverse osmosis membrane modified by two dimensional laminar MoS_2 with improved desalination performance and fouling-resistant characteristics, Desalination, 454 (2019) 48–58.

[22] L. Wang, N. Wang, J. Li, J. Li, W. Bian, S. Ji, Layer-by-layer self-assembly of polycation/GO nanofiltration membrane with enhanced stability and fouling resistance, Sep. Purif. Technol., 160 (2016) 123–131.

[23] N. Wang, S. Ji, G. Zhang, J. Li, L. Wang, Self-assembly of graphene oxide and polyeletrolyte complex nanohybrid membranes for nanofiltration and pervaporation, Chem. Eng. J., 213 (2012) 318–329.

[24] Y. Li, L. H. Wee, A. Volodin, J.A. Martens, I.F. Vankelecom, Polymer supported ZIF-8 membranes prepared via an inter facial synthesis method, Chem. Commun., 51 (2015) 918–920.

[25] H.P. Srivastava, G. Arthanareeswaran, N. Anantharaman, V. Starov, Performance of modified poly (vinylidene fluoride) membrane for textile wastewater ultra filtration, Desalination, 82 (2011) 87–94.

[26] S.U. Hong, M.L. Bruening, Separation of amion acid mixtures using multilayer polyelectrolyte nanofiltration membranes, J. Membr. Sci., 180 (2006) 1–5.

[27] L. Shan, H. Guo, Z. Qin, N. Wang, S. Ji, G. Zhang, Z. Zhang, Covalent cross linked polyelectrolyte complex membrane with high negative charges towards anti-natural organic matter fouling nanofiltration, RSC Adv., 5 (2015) 11515–11523.

[28] Q. Chen, P. Yu, W. Huang, S. Yu, M. Liu, C. Gao, High-flux composite hollow fiber nanofiltration membranes fabricated through layer-by-layer deposition of oppositely charged cross linked polyelectrolytes for dye removal, J. Membr. Sci., 492 (2015) 312–321.

[29] J. Appel, D. Li, J. Podlevsky, A. Debnath, A. Green, Q.H. Wang, J. Chae, Low cytotoxicity and genotoxicity of two-dimensional MoS_2 and WS_2, ACS Biomater. Sci. Eng., 2 (2014) 361–367.